Evolution of the Ca isotopic composition of the mantle

Elsa Amsellem, Frédéric Moynier, Igor S. Puchtel

Evolution of the Ca isotopic composition of the mantle

Elsa Amsellem[1], Frédéric Moynier[1,2], Igor S. Puchtel[3]

[1] Université de Paris, Institut de physique du globe de Paris, CNRS, F-75005 Paris, France
[2]Institut Universitaire de France, Paris, France.
[3]Department of Geology, University of Maryland, 8000 Regents Drive, College Park, MD 20742, USA.

Corresponding author:

Elsa Amsellem

email: amsellem@ipgp.fr

Revised for: GCA

Version: May 17, 2019

Abstract

Calcium stable isotopes are mainly fractionated during low-temperature geochemical processes and have, therefore, the potential to trace weathering and incorporation of recycled carbonated material in the mantle. However, behavior of Ca isotopes during mantle processes over Earth's history is not well understood. In this study, we present Ca isotopic compositions of 27 spinifex-textured and olivine cumulate komatiites ranging in age from 2.41 to 3.55 Ga. The Ca isotopic composition of all spinifex textured komatiites analyzed is similar, with an average $\delta^{44/40}Ca = 0.92 \pm 0.16‰$ (n=7; 2SD) (permil deviation of the $^{44}Ca/^{40}Ca$ ratio from SRM915a). This value is identical, within error, to the previous estimates of the composition of the mantle. In contrast, olivine cumulates from the Weltevreden Formation in the Barberton Greenstone Belt are isotopically heavier compared to the rest of the komatiites studied. While igneous processes and sea-floor alteration unlikely account for this Ca isotopic signature, crystallization of an early crust from a global magma ocean is a possibility, in agreement with previously obtained O, Os, Nd, Hf isotopic data and trace elements systematics.

1. Introduction

As a refractory element (Tc=1517° K, Lodders, 2003), Ca abundance and isotopic composition are not affected by volatility processes that may have occurred during the early stages of Earth's formation and evolution, in contrast to more volatile elements, such as Ga (Kato and Moynier, 2017) or even Si and Mg (Pringle et al. 2014; Hin et al., 2017). As a lithophile element, Ca is not segregated into the core and, therefore, its abundance and isotopic composition in the Bulk Silicate Earth (BSE) should be representative of the bulk Earth. On the other hand, Ca isotopes fractionate during mantle processes (e.g., Huang et al. 2010, Kang et al. 2016; 2017). This was first illustrated by up to ~0.2‰ differences between

45 the Ca isotopic composition (reported as $\delta^{44/40}$Ca, the permil deviation of the ^{44}Ca/^{40}Ca ratio
46 in a sample from that of the SRM915a standard) of peridotites and basalts, which is related to
47 either partial melting or fractional crystallization (e.g., Amini et al., 2009; Huang et al.,
48 2010;; Kang et al., 2016; Amsellem et al., 2017; Kang et al., 2017; Valdes et al., 2019).
49 Furthermore, Ca isotopes are highly fractionated under low temperature surface processes; in
50 particular, Ca is ~0.5‰ enriched in lighter isotopes in marine carbonates compared to basalts
51 (e.g., Gussone et al., 2005; Skulan et al., 1997; Skulan and DePaolo, 1999; Farkaš et al.,
52 2011; Fantle and Tipper, 2013; Schmitt et al., 2003; De La Rocha and DePaolo, 2000).
53 Calcium isotopes can, therefore, be used as tracers of carbonate contamination in the source
54 of magmatic rocks (e.g., Huang et al., 2011). However, these applications are limited by the
55 poor knowledge of the Ca isotopic composition of the modern terrestrial mantle and its
56 evolution through time due to recycling of subducted material, formation of the crust and/or
57 chemical exchange with the sub-lithospheric mantle. Furthermore, the composition of the
58 bulk silicate Earth (BSE) is central to inter-planetary comparisons (e.g., Simon and DePaolo,
59 2010, Valdes et al., 2014, Amsellem et al., 2017; Huang and Jacobsen, 2017).
60 The Ca isotopic composition of the BSE has been first estimated by Simon and
61 DePaolo (2010) and Huang et al. (2010) and, more recently, revisited by Kang et al. (2017).
62 Huang et al. (2010) measured the Ca isotopic composition of clinopyroxene and
63 orthopyroxene in two different mantle peridotites and, using the proportion of each mineral in
64 the mantle, estimated the BSE value to be $\delta^{44/40}$Ca = 1.05 ± 0.04‰. Simon and DePaolo
65 (2010) and more recently Simon et al. (2017), suggested that the similarity of measured
66 peridotites, basaltic rocks, and extraterrestrial samples reflect the BSE composition, which
67 after a ~0.1‰ correction to account for excess ^{40}Ca in the SRM915a standard (see Simon et
68 al., 2009; Mills et al., 2018) return(s?) a $\delta^{44/40}$Ca of 0.88 ± 0.07‰ (2sd). Kang et al. (2017)
69 focused their study on a large suite of peridotites xenoliths, both fertile and metasomatized.

70 Their estimate is slightly lighter than the one from Huang et al. (2010), with the $\delta^{44/40}$Ca
71 value of 0.94 ± 0.05‰.

72 The goal of the present study is to obtain new information on the behavior of Ca
73 isotopes during high temperature processes and to test whether the Ca isotopic composition
74 of the BSE varies through time via analyzing komatiites of various ages. Komatiites are
75 ultramafic volcanic rocks with >18% MgO. Most komatiites are Archean in age, although
76 there are rare occurrences in the Proterozoic (e.g., Hanski et al., 2004) and even Phanerozoic
77 (Echeverria, 1980). Nisbet et al. (1993) used komatiites to trace the evolution of the thermal
78 regime of the mantle through time. The origin of komatiites is generally related to anydrous
79 partial melting in hot mantle plumes (e.g., Campbell, 1989; Arndt et al., 2008), but alternative
80 scenarios also exist (e.g., hydrous melting in subduction zones, Grove and Parman, 2004).
81 Since komatiites are formed by 30 to 50% partial melting (Herzberg 1992), and Ca is an
82 incompatible element, it is enriched in the melt relative to the mantle residue. The almost
83 quantitative extraction of Ca, together with the fact that the melting occurred at high
84 temperatures, implies that Ca isotopic composition of komatiites is likely representative of
85 their mantle source. Therefore, komatiites are very useful for studies of the evolution of Ca
86 isotopic composition of the mantle through time, as was also previously shown for Ga, Sr,
87 Mg, Fe, Mo, Ti, Zn and Ni (Kato et al., 2017; Amsellem et al., 2018; Dauphas et al., 2010;
88 Greber et al., 2015; 2017; Sossi et al., 2018; Gall et al., 2017).

89 Here, we present the Ca isotopic composition of 27 komatiites ranging in age from
90 2.41 Ga to 3.55 Ga from South Africa, Fennoscandia, and Canada. We show that the Ca
91 isotopic composition of most komatiites overlap within error with the estimates of the
92 present-day BSE (0.94 ± 0.05 ‰, Kang et al. 2017 and 1.05 ± 0.04 ‰, Huang et al. 2010).
93 However, some samples show departure from this average with both light (down to 0.64 ±
94 0.03‰) and heavy (1.54 ± 0.09‰) Ca isotopic compositions. In particular, the olivine

cumulates from the Weltevreden formation in the Barberton Greenstone Belt and one cumulate sample from the Boston Creek in the Abitibi Greenstone Belt are enriched in the heavy Ca isotopes compared to the rest of the komatiites. We explore here the different processes that could produce these variations. The enrichment in the heavier Ca isotopes of the Weltevreden komatiites is suggested to originate from crystallization of an early terrestrial magma ocean, as was previously proposed for these komatiites by Puchtel et al. (2013; 2014) and Byerly et al. (2017).

2. Samples and Methods

2.1. Samples

A total of 27 komatiites (olivine and pyroxene spinifex-textured and olivine cumulates) were analyzed for Ca isotopic composition (Table 1). The komatiite samples from the Victoria's lava lake in the Vetreny Belt and the Kostomuksha Greenstone Belt in Fennoscandia, the Barberton Greenstone Belt (including the Komati and Weltevreden Formations and Schapenburg Greenstone Remnant) in South Africa, the Belingwe Greenstone Belt in Zimbabwe, and the Abitibi Greenstone Belt (the Boston Creek Flow) in Canada have previously been studied for trace element and HSE abundances and Pt-Re-Os, ^{142,143}Nd, ^{182}W isotope systematics by Puchtel et al. (2016a,b; 2013; 2014; 1998; 2001; 2005; 2018). All samples studied come from variably differentiated lava flows, with the spinifex-textured upper part and the olivine cumulate lower part. They all show features of seafloor alteration and/or metamorphic grade from prehnite-pumpellyite facies (Vetreny Belt, Boston Creek, Weltevreden) to greenschist-amphibolite facies (Schapenburg, Kostomuksha and Komati). In some of the komatiites (Schapenburg, Kostomuksha, Boston Creek), most olivines have been altered to serpentine, chlorite and/or magnetite and some of the pyroxenes have been altered to tremolite and chlorite. Vetreny Belt komatiites have assimilated up to

4% crustal rocks (Puchtel et al., 1996; 2016a). The komatiites studied here are classified as both Al-depleted/enriched (Schapenburg, Komati, Weltevreden, Kostomuksha, Boston Creek) and Al-undepleted (Belingwe, Vetreny). Olivine cumulate samples present an average composition of olivine between 30% to 50% for Kostomuksha, 50% for Belingwe and 60% for Barberton (Puchtel and Humayun, 2005; Puchtel et al., 2009b; Puchtel et al., 2013).

2.2. Analytical techniques

Between 15 to 30 mg of sample powder was digested in a HNO_3/HF mixture (1:3) on a hot plate at 120 °C for 48 h. When dried down, 2 mL of 6N HCl were added to the sample residues to destroy any fluoride phases. Calcium was seperated from the matrix using DGA extraction chromatography resin and Sr-selective extraction chromatographic resin following the protocol described in Valdes et al. (2014) and Amsellem et al. (2017). Calcium was first eluted with Sr using 1.8 mL of DGA resin in concentrated HNO_3 and was afterwards eluted on 200 µL of 20-50 µm of Sr-selective extraction chromatographic resin in 3N HNO_3 to separate it from Sr. Final Ca cuts were dried down and redissolved in 0.1 N HNO_3 for mass spectrometric analysis.

The Ca isotopic composition was measured using a *ThermoFischer* Netpune multi-collector inductively-coupled plasma mass-spectrometer (MC-ICPMS) at the Institut de Physique du Globe de Paris. Samples were introduced with a desolvating Apex nebulizer at an aspiration rate of 50 $\mu L \times min^{-1}$. Each analysis included 20 cycles with an integration time of 8.389 s. The intensity of the ion beams on the masses 42, 43 and 44 were measured and $^{42}Ca/^{44}Ca$ and $^{43}Ca/^{44}Ca$ ratios were calculated. Measurements were run in high resolution slit mode with a mass resolution of R~6350. Calcium isotopic variations are defined here in per mil units and using the $^{44}Ca/^{40}Ca$ ratio: $\delta^{44/40}Ca = (((^{44}Ca/^{40}Ca)_{sample}/(^{44}Ca/^{40}Ca)_{standard})-1) \times 1000$ to facilitate comparison with literature data by converting the results using the mass-dependent fractionation law: $\delta^{44/40}Ca = -1.974 \times \delta^{42/44}Ca$ after making sure that the data were

mass-dependent. The standard bracketing method (with NIST SRM 915b as the standard) was used for correcting for mass-fractionation during the analysis. The Ca isotopic composition was re-normalized to SRM 915a using the isotopic composition of SRM 915a relative to SRM 915b from Valdes et al. (2014) of -0.71‰ for $\delta^{44/40}$Ca. The analytical uncertainty was calculated from repeated measurements of the same solutions and is defined as the 2SE to be 0.05‰.

3. Results

Calcium isotopic compositions of komatiites from this study are reported in Table 1 and presented in Figure 1. The $\delta^{44/40}$Ca values range from 0.64 ± 0.03 ‰ to 1.54 ± 0.09 ‰ averaging 1.03 ± 0.46 ‰ (2SD n=27). These values overlap with previously reported data for two 89 Ma Gorgona Island komatiites ($\delta^{44/40}$Ca= 0.77 ± 0.06‰ and 0.61 ± 0.06‰) and two 3.5 Ga komatiites from the Onverwacht Group in South Africa ($\delta^{44/40}$Ca= 1.03 ± 0.05‰ and 0.98 ± 0.04‰) (Amini et al., 2009). The $\delta^{44/40}$Ca values obtained in this study are also similar to those in peridotites (ranging from ~0.9 to ~1.2, Amini et al., 2009; Kang et al., 2016; 2017; Amsellem et al., 2017; Zhao et al., 2017) as well as to most igneous rocks (~0.9, e.g., Amini et al., 2009; Simon and DePaolo, 2010; Valdes et al., 2014; Amsellem et al., 2017; Simon et al., 2017).

The Ca isotopic compositions of the spinifex-textured samples are less scattered than those of the olivine cumulate komatiites, and cluster around the BSE estimate ($\delta^{44/40}$Ca= 0.92 ± 0.16 ‰, 2SD n=7). In contrast, the 5 olivine cumulates from the Weltevreden Formation and Boston Creek are enriched in the heavier Ca isotopes ($\delta^{44/40}$Ca ranges from 1.33 ± 0.05‰ to 1.54 ± 0.09‰), whereas one Kostomuksha olivine cumulate is depleted in the heavier isotopes ($\delta^{44/40}$Ca = 0.64 ± 0.03‰).

4. Discussion

4.1 The evolution of the $\delta^{44/40}$Ca of the bulk silicate Earth through time

On average, irrespective of ages and locations, spinifex-textured komatiites have isotopic compostions (from $\delta^{44/40}$Ca = 0.83 ± 0.03‰ to $\delta^{44/40}$Ca = 1.06 ± 0.05‰) similar to the estimates for the BSE's (0.88 ± 0.07‰, 1.05 ± 0.04‰ and 0.94 ± 0.05‰) based on the data for peridotites (Simon and DePaolo, 2010; Huang et al., 2010 and Kang et al., 2017). Since spinifex-textured komatiites crystallized relatively quickly and experienced little fractionation after emplacement (Donaldson, 1976), they are usually taken as the next best samples (with the chilled margin samples being the best) to represent the composition of the emplaced komatiite lava. Hence, among the samples analyzed, the spinifex-textured komatiites are expected to best represent the Ca isotopic composition of the mantle. The variability observed in the olivine cumulates will be discuss in a different section.

Komatiites formed via high degrees of partial melting, and Ca, as an incompatible element, was mostly incorporated into the melt, limiting the effect of isotopic fractionation during melt extraction. Hence, komatiites are reliable samples of Ca isotopic composition of the Archean mantle. Since spinifex-textured komatiites represent nearly the original liquid composition, in order to estimate the Ca isotopic composition of the BSE, only spinifex-textured komatiites were used. As such, 7 komatiite samples were chosen including the 2.72 Ga Boston Creek, 2.82 Ga Kostomuksha, and the 3.55 Ga Schapenburg komatiites. These komatiites do not show any resolvable Ca isotopic variations with emplacement age, ranging from $\delta^{44/40}$Ca = 0.83 ± 0.03‰ to $\delta^{44/40}$Ca = 1.06 ± 0.05‰, implying that the extraction of the continental crust from the mantle over the 800 Ma of Earth's history did not have an effect on the Ca isotopic composition of the komatiites sources.

When averaged together, these samples yield a mean $\delta^{44/40}$Ca value of 0.92 ± 0.16‰ (2SD n=7) which is indistinguishable from the estimated composition of the BSE (0.88 ±

195 0.07‰,1.05 ± 0.04‰ and 0.94 ± 0.05‰, Simon and DePaolo, 2010; Huang et al. 2010 and
196 Kang et al. 2017, respectively).
197
198 **4.2 Effects of crustal assimilation and post-emplacement isotopic fractionation**
199 **on the Ca isotopic composition of the komatiites**
200 Assimilation of crustal material has been shown to have occurred in some komatiites
201 (e.g., Cattell, 1987; Arndt and Jenner, 1986) and this could have potentially modified the Ca
202 isotopic composition of the original melt. However, some crustal rocks (granites: $\delta^{44/40}$Ca=
203 ~0.8‰, Gussone et al., 2016) have slightly lighter Ca isotopic composition compared to
204 peridotites and most of the komatiites studied, as well as lower Ca abundances (< 2 wt%, e.g.,
205 Marshall and DePaolo, 1989). As such, crustal contamination would have shifted Ca isotopic
206 composition of the komatiites in the opposite direction, and, therefore, cannot be responsible
207 for their heavier Ca isotopic composition. Moreover, mass-balance calculations indicate that,
208 in order to account for the lightest Ca isotopic composition of the komatiites (~0.8‰, Table
209 1), more than 50% crustal material (granites) needs to be assimilated by the komatiitic
210 parental magma, which is not observed in any of the komatiites studied based on trace
211 element and isotopic data. The effect on Ca isotopes of a post-emplacement crustal
212 assimilation through a mixture of basalts and sediments is more difficult to estimate
213 regarding the variability of $\delta^{44/40}$Ca in sediments, depending on the location and the type of
214 sediments. However, the degree of contamination via this process is unlikely to exceed 10%
215 (Huppert et al., 1984). In any way, the only komatiites in this study that were shown to have
216 undergone ca. 4% crustal assimilation, the Vetreny Belt komatiites (Puchtel et al., 1996;
217 2016a), show a range of $\delta^{44/40}$Ca from 0.89 ± 0.06‰ to 1.06 ± 0.11‰, which overlaps with
218 that for the fertile peridotites from Kang et al. (2017). Therefore, we conclude that there is

219 little to no evidence that crustal assimilation affected the Ca isotopic composition of the
220 parental komatiitic magmas.

221 Post-magmatic alteration is another process that may have modified the primary Ca
222 isotopic composition of the komatiites (e.g., John et al., 2012; Hindshaw et al., 2013;
223 Jacobson et al., 2015). Among the samples studied here, komatiites from the Schapenburg
224 and Munro Township localities show evidence of CaO loss during serpentinization (Puchtel
225 et al., 2009a; 2009b). Both the Komati and Weltevreden formations of the Barberton
226 Greenstone Belt have undergone seafloor alteration and CaO was affected by secondary
227 processes (Puchtel et al., 2013). Furthemore, Puchtel et al. (1998) showed that in the
228 Kostomuksha komatiites, CaO was mobile during alteration and preferentially removed from
229 the samples with high modal olivine contents (corresponding to the cumulate samples). This
230 is consistent with the negative correlation between CaO content and loss on ignition (LOI)
231 observed in some komatiites (Boschi et al., 2008). Albitization of plagioclase during
232 serpentinization results in the incorporation of Na in the calcic plagioclase of the crust and
233 the removal of Ca from the plagioclase to the fluid.

234 Serpentinization has been suggested to result in a decrease in the $\delta^{44/40}$Ca (John et al.,
235 2012) and this process may explain the composition of the isotopically light Kostomuksha
236 sample (see Figure 1). Figure 2 presents the Ca isotopic compostion and the CaO abundance
237 of the komatiites relative to their LOI determined previously (Puchtel et al., 1998; 2013;
238 2016a; 2016b and 2018). In the komatiite samples with up to 6% LOI, CaO concentration and
239 Ca isotopic composition are constant, whereas in samples with LOI > 6%, CaO
240 concentrations generally decrease, while the $\delta^{44/40}$Ca of the Kostomuksha samples decreases
241 and the $\delta^{44/40}$Ca of the 5 early Archean olivine cumulates from the Weltevreden and Boston
242 Creek localities increases. Therefore, the light Ca isotopic composition of the Kostomuksha
243 komatiite sample 94100 (LOI = 10.1%) is likely related to serpentinization. On the other

hand, the heavy Ca isotope composition of the Weltevreden and Boston Creek olivine cumulates cannot be explained by serpentinization (John et al., 2012). It is more likely to be related to another process (e.g., differences in the source compositions, partial melting, accumulation of isotopically heavy olivine, etc., see below).

Another way to monitor the effect of alteration is to use the ratio of Ca over an immobile element during alteration processes, such as Zr. CaO/Zr ratio does not correlate with $\delta^{44/40}$Ca (Figure 3), indicating that the heavy Ca isotopic compositions of the Weltevreden and Boston Creek komatiites are not due to secondary processes alone. The Ca content in komatiites is dominated by the amount of interstitial liquid and products of its crystallization (e.g., pyroxene and plagioclase). In the Weltevreden cumulates, olivine grains (CaO~0.24%) are surrounded by interstitial magmatic pyroxene, mostly augite (CaO~10%). In all komatiites, the Ca content strongly correlates with the Zr content (Figure 4) implying that the Ca content reflects igneous processes, assimilation or source effects and not secondary alteration as Zr is insoluble in aqueous fluids.

4.3 Primordial magma ocean processes recorded in the heavy Ca isotopic composition of the Weltevreden komatiites?

The olivine cumulate samples of the Weltevreden Formation from the Barberton Greenstone Belt have the heaviest Ca isotopic composition of all komatiites studied, averaging 1.47 ± 0.11‰. These heavy signatures were observed for dunites (Amini et al., 2009; Huang et al., 2010) and wehrlites (Ionov et al., 2018) which are likely due to their petrology with a low content of Ca. The dunite and wehrlite present the highest content of olivine in peridotites thus, this isotopic signature could rather be related to equilibrium isotopic fractionation between olivine and melt as olivine is enriched in the heavier isotopes of Ca (~1.16‰) compared to clinopyroxenes (~0.9‰); $\Delta^{44/40}Ca_{ol\text{-}cpx}\approx0.3‰$ (Kang et al.,

2016). Huang et al. (2019) have estimated the fractionation factor between forsterite (the main liquidus mineral in komatiites) and diopside (the main Ca-bearing mineral phase in komatiites) to be up to 0.9‰ at 1000K. However, the fractionation factor decreases considerably with the temperature and komatiitic magmas can reach liquidus temperatures of up to 1600 °C (e.g., Puchtel et al., 2013). The difference of ~0.5‰ between olivine cumulate and olivine spinifex might thus be difficult to reconcile with fractional crystallization. Moreover, there is no corelation between the olivine content in the cumulates with their Ca isotopic composition. This is consistent with the absence of fractionation during differenciation observed in Kilauea Iki Lava lake samples (Zhang et al., 2018) and in the homogeneity in different type of mantle rocks (Chen et al., 2019). In addition, the enrichment of the heavier isotopes is not systematic for all cumulates, since Weltevreden komatiites are the only ones enriched in the heavier Ca isotopes.

Weltevreden komatiites might be unique and would have been generated under different conditions compared to other komatiites. This is illustrated by the olivines from the Weltevreden formation samples that are enriched in the lighter O isotopes compared to other komatiites and other volcanic rocks (Byerly et al., 2017). These authors show that the low $\delta^{18}O$ reflect that of the mantle source of these komatiites that was affected by fractionation of mineral phases stable under the magma ocean conditions, during transition from silicate to metal oxide phases, as oxygen isotope composition can be modified by up to 1.5‰ during this type of fractionation (Zheng, 1997).

The Weltevreden komatiite source shows highly positive initial εHf and near-zero initial εNd value which plot off the Nd-Hf terrestrial evolution array (Puchtel et al., 2013). To explain this decoupling, an early depleted reservoir that was isolated from a primordial magma ocean was suggested by these authors; this reservoir was characterized by Hf-Nd relationships different from those of the upper mantle. In addition, the initial $\varepsilon^{186}Os$ and

γ^{187}Os values of these komatiites defined a different evolution trend from chondritic paths, implying an early isolation of deep mantle domains (Puchtel et al., 2014). These domains are thought to represent the early products of crystallization of a magma ocean located at the bottom of the lower mantle (Abe, 1997) and were likely derived from the residual liquid separated during crystallization of the magma ocean, with Mg- and Ca-perovskites as fractionating phases suggested by melting experiments (e.g., Ito et al., 2004; Wood et al., 2000; Ringwood et al., 1970). Fractionation of light Ca isotopes in Ca-perovskite vs. pyroxene is consistent with these observations. Under equilibrium conditions, phases with the shortest Ca-O bond (i.e. lower coordination number) tend to be enriched in the heavier Ca isotopes (Huang et al., 2010). Calcium in Ca-perovskite has the highest coordination number (CN=12) compared to other Ca-bearing minerals (CN<10; Smyth and Bish, 1988 and Sowrey et al., 2004). Cumulate should, therefore, be enriched in lighter Ca isotopes leading to the residual liquid with heavier Ca isotopic composition, which is indeed observed in the Weltevreden komatiites. If the heavy Ca isotopic composition of the Weltevreden komatiites is due to mantle heterogeneity following magma ocean crystallization, the question is why the Komati komatiites are not isotopically heavy as well. A possibility would be that they do not sample the same source, as suggested by εHf data, which reflect the difference of Ca isotopic composition (Figure 5). As Komati samples are older than the Weltevreden komatiites, the residual liquid representing the source of Weltevreden komatiites would record a longer history of crystallization producing an isotopically heavier source. This is consistent with the estimates for the proportions of Ca- and Mg-perovskite that crystallized to form the mantle domains that later gave rise to the Komati and Weltevreden komatiites (30% and 40% crystallization, respectively). To estimate the evolution of Ca isotopic composition of the residual liquid representing the sources for the Barberton komatiites from the crystallization of the magma ocean, we use a Rayleigh distillation equation.

$$\delta Ca_{melt} = (\delta Ca_{initial\ melt} + 1000)f^{(\alpha-1)} - 1000$$

Where f represents the fraction of Ca remaining in the melt and α represents the isotopic fractionation factor between the crystals and the melt. We consider 5 different values of α representing a fractionation between the crystals and the melt ranging from 0.1‰ to 0.5‰ which would be expected in equilibrium fractionation due to their different coordination number. The $\delta Ca_{inital\ melt}$ is set to be 1‰. The results of the modeling are shown in Figure 6. In order to explain the data for the Weltevreden and Komati komatiites, between 10% and 50% of the Ca remains in the melt for the former and between 50% and 90% for the latter. Considering the silicate perovskite melt partitioning of Ca, which is estimated to be between $D_{Capv\text{-}melt}$= 3 and 4 under the lower mantle conditions (Corgne et al., 2005), and using the crystallization fractionation law, we predict a difference of at least 10% in the degree of crystallization between the source of Komati and Weltevreden komatiites where the source of Weltevreden komatiites would have been affected by more crystallization, consistent with the results from Puchtel et al. (2013). Furthermore, during perovskite partitioning in a magma, Nb/Ta and Zr/Hf ratios are expected to correlate because of the difference of compatibility of these elements in perovskite (Chakhmouradian et al., 2013). This is observed for Barberton komatiites (Figure 7a) and the Ca isotopic composition correlates with Nb/Ta (Figure 7b). These results can explain the variability in Ca isotopic composition between the Komati and Weltevreden komatiites and suggest that the residual liquid of the source of the latter was more affected by crystallization.

Conclusions

The Ca isotopic composition of 27 spinifex-textured and cumulate komatiites from around the globe, ranging in age between 2.41 and 3.48 Ga, has been analyzed. The spinifex-textured komatiites have similar isotopic compositions averaging at 0.92 ± 0.16‰,

indistiguishable from the previous estimates for the BSE composition derived from peridotites (Huang et al., 2010; Kang et al., 2017). Furthermore, the Ca isotopic composition of the Archean mantle has been shown to have been identical to that of the modern mantle.

Olivine cumulate komatiites from the 3.26 Ga Weltevreden Formation of the Barberton Greenstone Belt are strongly enriched in the heavier Ca isotopes compared to the other komatiites studied. When considered together with the available O, Os, Nd, and Hf isotopic data for these rocks (Byerly et al., 2017; Puchtel et al., 2013, 2014), magma ocean processes appear to be the most likely mechanism to explain the Ca isotopic composition of these komatiites.

Acknowledgements

FM acknowledges funding from the European Research Council under the H2020 framework program/ERC grant agreement #637503 (Pristine) and financial support of the UnivEarthS Labex program at Sorbonne Paris Cité (ANR-10-LABX- 0023 and ANR-11-IDEX-0005-02), and the ANR through a chaire d'excellence Sorbonne Paris Cité. We thank Pascal Louvat for providing help during Ca isotopic measurement with the *Neptune*. ISP would like to thank Euan Nisbet and Gary Byerly for sharing their collections of Belingwe, Komati and Weltevreden komatiites. The original version of this manuscript benefitted from thorough reviews by Justin Simon, Martin Schiller and an anonymous reviewer. We thank AE Shichun Huang for editorial handling of the manuscript and scientific comments.

References

Abe, T. (1997) Thermal and chemical evolution of the terrestrial magma ocean. *Phys. Earth Planet. Inter.* **100**, 27–39.

Amini M., Eisenhauer A., Böhm F., Holmden C., Kreissig K., Hauff F. and Jochum K. P. (2009) Calcium isotopes ($\delta^{44/40}$Ca) in MPI-DING reference glasses, USGS rock powders and various rocks: Evidence for Ca isotope fractionation in terrestrial silicates. *Geostand. Geoanalytical Res.* **33**, 231-247.

Amsellem E., Moynier F., Pringle E. A., Bouvier A., Chen H. and Day J. M. D. (2017) Testing the chondrule-rich accretion model for planetary embryos using calcium isotopes. *Earth Planet. Sci. Lett.* **469**, 75–83.

Amsellem E., Moynier F., Day J. M. D., Moreira M., Puchtel I. S. and Teng F.-Z. (2018) The stable strontium isotopic composition of ocean island basalts, mid-ocean ridge basalts, and komatiites. *Chem. Geol.* **483**, 595-602.

Arndt N. T. and Jenner G. A. (1986) Crustally contaminated komatiites and basalts from Kambalda, Western Australia. *Chem. Geol.* **56**, 229-255.

Arndt N. T., Lesher C. M. and Barnes S. J. (eds) (2008). Komatiite. Cambridge University Press, 488 pp.

Boschi C., Dini A., Früh-Green G. L. and Kelley D. S. (2008) Isotopic and element exchange during serpentinization and metasomatism at the Atlantis Massif (MAR 30°N): Insights from B and Sr isotope data. *Geochim. Cosmochim. Acta* **72**, 1801–1823.

Byerly B. L., Kareem K., Bao H. and Byerly G. R. (2017) Early Earth mantle heterogeneity revealed by light oxygen isotopes of Archaean komatiites. *Nat. Geosci.* **10**, 871–875.

Campbell I. H., Griffiths R. W and Hill, R. I. (1989) Melting in an Archean mantle plume : heads it's basalts, tails it's komatiites. *Nature* **339**, 697-699.

Cattell A. (1987) Enriched komatiitic basalts from Newton Township, Ontario : their genesis by crustal contamination of depleted komatiite magma. *Geol. Mag.* **124**, 303-309.

Chakhmouradian, A. R., Reguir, E. P., Kamenetsky, V. S., Sharygin, V. V. and Golovin, A. V. (2013) Trace-element partitioning in perovskite : Implications for the geochemistry of kimberlites and other mantle-derived undersaturated rocks. *Chem. Geol*. **353**, 112-131.

Chen C., Dai W., Wang Z., Liu Y., Li M., Becker H. and Foley S. F. (2019) Calcium isotope fractionation during magmatic processes in the upper mantle. *Geochim. Cosmochim. Acta* **249**, 121-137.

Corgne, A. & Wood, B. J. (2005) Trace element partitioning and substitution mechanisms in calcium perovskites. *Contrib. Mineral. Petrol.* **149**, 85–97.

Dauphas N., Teng F. Z. and Arndt N. T. (2010) Magnesium and iron isotopes in 2.7 Ga Alexo komatiites: Mantle signatures, no evidence for Soret diffusion, and identification of diffusive transport in zoned olivine. *Geochim. Cosmochim. Acta* **74**, 3274–3291.

De La Rocha C. L. and DePaolo D. J. (2000) Isotopic Evidence for Variations in the Marine Calcium Cycle Over the Cenozoic. *Science* **289**, 1176–1178.

Donaldson C. H. (1976) An experimental investigation of olivine morphology. *Contrib. to Mineral. Petrol.* **57**, 187–213.

Echeverria L. M. (1980) Tertiary or Mesozoic Komatities from Gorgona Island: fields relations and geochemistry. *Contrib. to Mineral. Petrogr.* **73**, 253–266.

Fantle M. S. and Tipper E. T. (2014) Calcium isotopes in the global biogeochemical Ca cycle: Implications for development of a Ca isotope proxy. *Earth-Science Rev.* **129**, 148–177.

Farkaš J., Déjeant A., Novák M. and Jacobsen S. B. (2011) Calcium isotope constraints on the uptake and sources of Ca^{2+} in a base-poor forest: A new concept of combining stable ($\delta^{44/42}Ca$) and radiogenic (εCa) signals. *Geochim. Cosmochim. Acta* **75**, 7031–7046.

Gall L., Williams H. M., Halliday A. N. and Kerr A. C. (2017) Nickel isotopic composition of the mantle. *Geochim. Cosmochim. Acta* **199**, 196–209.

Greber N. D., Puchtel I. S., Nägler T. F. and Mezger K. (2015) Komatiites constrain molybdenum isotope composition of the Earth's mantle. *Earth Planet. Sci. Lett.* **421**, 129–138.

Greber N. D., Dauphas N., Bekker A., Ptáček M. P., Bindeman I. N. and Hofmann A. (2017) Titanium isotopic evidence for felsic crust and plate tectonics 3.5 billion years ago. *Science* **357**, 1271–1274.

Grove T. L. and Parman S. W. (2004) Thermal evolution of the Earth as recorded by komatiites. *Earth Planet. Sci. Lett.* **219**, 173–187.

Gussone N., Böhm; F., Eisenhauer A., Dietzel M., Heuser A., Teichert B. M. A., Reitner J., Wörheide G. and Dullo W. C. (2005) Calcium isotope fractionation in calcite and aragonite. *Geochim. Cosmochim. Acta* **69**, 4485–4494.

Gussone N., Schmitt A.-D., Heuser A., Wombacher F., Dietzel M., Tipper E. and Schiller M. (2016) *Calcium Stable Isotope Geochemistry*. Springer-Verlag Berlin Heidelberg.

Hanski E., Walker R. J., Huhma H., Polyakov G. V., Balykin P. A., Hoa T. T. and Phuong N. T. (2004) Origin of the Permian-Triassic komatiites, northwestern Vietnam. *Contrib. to Mineral. Petrol.* **147**, 453–469.

Herzberg C. (1992) Depth and degree of melting of komatiites. *J. Geophys. Res.* **97**, 4521-4540.

Hin R. C., Coath C. D., Carter P. J., Nimmo F., Lai Y.-J., Pogge von Strandmann P. A. E., Willbold M., Leinhardt Z. M., Walter M. J. and Elliott T. (2017) Magnesium isotope evidence that accretional vapour loss shapes planetary compositions. *Nature* **549**, 511–515.

Hindshaw R. S., Bourdon B., Pogge von Strandmann P. A. E., Vigier N. and Burton K. W. (2013) The stable calcium isotopic composition of rivers draining basaltic catchments in Iceland. *Earth Planet. Sci. Lett.* **374**, 173–184.

Huang F., Zhou C., Wang W., Kang J. and Wu Z. (2019) First-principles calculations of equilibrium Ca isotope fractionation : Implications for oldhamite formation and evolution of lunar magma ocean. *Earth Planet. Sci. Lett.* **510**, 153-160.

Huang S. and Jacobsen S. B. (2017) Calcium isotopic composition of chondrites. *Geochim. Cosmochim. Acta* **201**, 364-376.

443 Huang S., Farkaš J. and Jacobsen S. B. (2011) Stable calcium isotopic compositions of
444 Hawaiian shield lavas: Evidence for recycling of ancient marine carbonates into the mantle.
445 *Geochim. Cosmochim. Acta* **75**, 4987–4997.

446 Huang S., Farkaš J. and Jacobsen S. B. (2010) Calcium isotopic fractionation between
447 clinopyroxene and orthopyroxene from mantle peridotites. *Earth Planet. Sci. Lett.* **298**, 337-
448 344.

449 Huppert H. E., Sparks R. S. J., Turner S. and Arndt N. T. (1984) Emplacement and cooling of
450 komatiite lavas. *Nature* **309**, 19-22.

451 Ionov D. A., Qi Y-H., Kang J-T., Golovin A. V., Oleinikov O. B., Zheng W., Anbar A. D.,
452 Zhang Z-F., and Huang F. (2019) Calcium isotopic signatures of carbonatite and silicate
453 metasomatism, melt percolation and crustal recycling in the lithospheric mantle. *Geochim.*
454 *Cosmochim Acta* **248**, 1-13.

455 Ito, E., Kubo, A., Katsura, T. & Walter, M. J. (2004) Melting experiments of mantle
456 materials under lower mantle conditions with implications for magma ocean differentiation.
457 *Phys. Earth Planet. Inter.* **143–144**, 397-406.

458 Jacobson A. D., Grace Andrews M., Lehn G. O. and Holmden C. (2015) Silicate versus
459 carbonate weathering in Iceland: New insights from Ca isotopes. *Earth Planet. Sci. Lett.* **416**,
460 132–142.

461 John T., Gussone N., Podladchikov Y. Y., Bebout G. E., Dohmen R., Halama R., Klemd R.,
462 Magna T. and Seitz H. M. (2012) Volcanic arcs fed by rapid pulsed fluid flow through
463 subducting slabs. *Nat. Geosci.* **5**, 489–492..

464 Kang J. T., Zhu H. L., Liu Y. F., Liu F., Wu F., Hao Y. T., Zhi X. C., Zhang Z. F. and Huang
465 F. (2016) Calcium isotopic composition of mantle xenoliths and minerals from Eastern
466 China. *Geochim. Cosmochim. Acta* **174**, 335–344.

467 Kang J. T., Ionov D. A., Liu F., Zhang C. L., Golovin A. V., Qin L. P., Zhang Z. F. and
468 Huang F. (2017) Calcium isotopic fractionation in mantle peridotites by melting and
469 metasomatism and Ca isotope composition of the Bulk Silicate Earth. *Earth Planet. Sci. Lett.*
470 **474**, 128–137.

471 Kato C., Moynier F., Foriel J., Teng F. Z. and Puchtel I. S. (2017) The gallium isotopic
472 composition of the bulk silicate Earth. *Chem. Geol.* **448**, 164–172.

473 Kato C. and Moynier F. (2017) Gallium isotopic evidence for the fate of moderately volatile
474 elements in planetary bodies and refractory inclusions. *Earth Planet. Sci. Lett.* **479**, 330–339.

475 Lodders K. (2003) Solar System Abundances and Condensation Temperatures of the
476 Elements. *Astrophys. J.* **591**, 1220-1247

477 Marshall B. D. and DePaolo D. J. (1989) Calcium isotopes in igneous rocks and the origin of
478 granite. *Geochim. Cosmochim. Acta* **53**, 917–922.

Mills, R. D., Simon, J. I. and DePaolo, D. J. (2018) Calcium and neodynium radiogenic isotopes of igneous rocks : Tracing crustal contributions in felsic magmas related to super-eruptions and continental rifting. *Earth Planet. Sci. Lett.* **495**, 242-250.

Nisbet E. G., Arndt N. T., Bickle M. J., Cameron W. E., Chauvel C., Cheadle M., Hegner E. T. K. Kyser., Martin A., Renner R and Roedder E. (1987) Uniquely fresh 2.7Ga komatiites from the Belingwe greenstone belt, Zimbabwe. *Geology* **15**, 1147-1150.

Nisbet E. G., Cheadle M. J., Arndt N. T. and Bickle M. J. (1993) Constraining the Potential Temperature of the Archean Mantle - a Review of the Evidence from Komatiites. *Lithos* **30**, 291–307.

Pringle E. A., Moynier F., Savage P. S., Badro J. and Barrat J.-A. (2014) Silicon isotopes in angrites and volatile loss in planetesimals. *Proc. Natl. Acad. Sci.* **111**, 17029–17032.

Puchtel I. S., Hofmann A. W., Mezger · K, Shchipansky A. A., Kulikov V. S. and Kulikova V. V (1996) Petrology of a 2.41 Ga remarkably fresh komatiitic basalt lava lake in Lion Hills, central Vetreny Belt, Baltic Shield. *Contrib. to Miner. Pet.* **124**, 273–290.

Puchtel I. S., Haase K. M., Hofmann A. W., Chauvel C., Kulikov V. S., Garbe-Sch~nberg C.-D. and Nemchin ' A. A. (1997) Petrology and geochemistry of crustally contaminated komatiitic basalts from the Vetreny Belt, southeastern Baltic Shield: Evidence for an early Proterozoic mantle plume beneath rifted Archean continental lithosphere. *Geochim. Cosmochim. Acta* **61**, 1205–1222.

Puchtel I. S., Hofmann A. W., Mezger K., Jochum K. P., Shchipansky A. A. and Samsonov A. V. (1998) Oceanic plateau model for continental crustal growth in the Archaean: A case study from the Kostomuksha greenstone belt, NW Baltic Shield. *Earth Planet. Sci. Lett.* **155**, 57–74.

Puchtel I. S., Brügmann G. E. and Hofmann A. W. (2001) 187 Os-enriched domain in an Archean mantle plume: Evidence from 2.8 Ga komatiites of the Kostomuksha Greenstone Belt, NW Baltic Shield. *Earth Planet. Sci. Lett.* **186**, 513-526.

Puchtel I. S., Brandon A. D., Humayun M. and Walker R. J. (2005) Evidence for the early differentiation of the core from Pt-Re-Os isotope systematics of 2.8-Ga komatiites. *Earth Planet. Sci. Lett.* **237**, 118–134.

Puchtel I. S. and Humayun M. (2005) Highly siderophile element geochemistry of 187Os-enriched 2.8 Ga Kostomuksha komatiites, Baltic Shield. *Geochim. Cosmochim. Acta* **69**, 1607–1618.

Puchtel I. S., Walker R. J., Anhaeusser C. R. and Gruau G. (2009a) Re-Os isotope systematics and HSE abundances of the 3.5 Ga Schapenburg komatiites, South Africa: Hydrous melting or prolonged survival of primordial heterogeneities in the mantle? *Chem. Geol.* **262**, 391–405.

Puchtel I. S., Walker R. J., Brandon A. D. and Nisbet E. G. (2009b) Pt-Re-Os and Sm-Nd isotope and HSE and REE systematics of the 2.7 Ga Belingwe and Abitibi komatiites. *Geochim. Cosmochim. Acta* **73**, 6367–6389.

Puchtel I. S., Blichert-Toft J., Touboul M., Walker R. J., Byerly G. R., Nisbet E. G. and Anhaeusser C. R. (2013) Insights into early Earth from Barberton komatiites: Evidence from lithophile isotope and trace element systematics. *Geochim. Cosmochim. Acta*. **108**, 63-90.

Puchtel I. S., Walker R. J., Touboul M., Nisbet E. G. and Byerly G. R. (2014) Insights into early Earth from the Pt-Re-Os isotope and highly siderophile element abundance systematics of Barberton komatiites. *Geochim. Cosmochim. Acta* **125**, 394–413.

Puchtel I. S., Touboul M., Blichert-Toft J., Walker R. J., Brandon A. D., Nicklas R. W., Kulikov V. S. and Samsonov A. V. (2016) Lithophile and siderophile element systematics of Earth's mantle at the Archean-Proterozoic boundary: Evidence from 2.4 Ga komatiites. *Geochim. Cosmochim. Acta* **180**, 227–255.

Puchtel I. S., Blichert-Toft J., Touboul M. Horan, M.F and Walker R. J. (2016) The couples ^{182}W-^{142}Nd record of early terrestrial mantle differentiation. Geochem. Geophys. Geosyst. **17**, 2168–2193.

Puchtel I. S., Blichert-Toft J., Touboul M. and Walker R. J. (2018) ^{182}W and HSE constraints from 2.7 Ga komatiites on the heterogeneous nature of the Archean mantle. *Geochim. Cosmochim. Acta* **228**, 1–26.

Ringwood, A. E. (1970) Phase transformations and the constitution of the mantle. *Phys. Earth Planet. Inter*. **3**, 109–155.

Schmitt A. D., Chabaux F. and Stille P. (2003) The calcium riverine and hydrothermal isotopic fluxes and the oceanic calcium mass balance. *Earth Planet. Sci. Lett.* **213**, 503–518.

Skulan J., DePaolo D. J. and Owens T. L. (1997) Biological control of calcium isotopic abundances in the global calcium cycle. *Geochim. Cosmochim. Acta* **61**, 2505–2510.

Skulan J. and DePaolo D. J. (1999) Calcium isotope fractionation between soft and mineralized tissues as a monitor of calcium use in vertebrates. *Proc. Natl. Acad. Sci.* **96**, 13709–13713.

Smyth J.R. and Bish D.L. (1988) *Crystal structures and cations sites of rock-forming minerals*. Allen and Unwin, Boston.

Sossi P. A., Nebel O., O'Neill H. S. C. and Moynier F. (2018) Zinc isotope composition of the Earth and its behaviour during planetary accretion. *Chem. Geol.* **477**, 73–84.

Sowrey F.E., Skipper L.J., Pickup D.M., Drake K.O., Lin Z., Smith M.E. and Newport R.J. (2004) Systematic empirical analysis of calcium-oxygen coordination environment by calcium K-edge XANES. Phys. Chem. Chem. Phys. **6**, 188-192.

Simon J. I. and DePaolo D. J. (2010) Stable calcium isotopic composition of meteorites and rocky planets. *Earth Planet. Sci. Lett.* **289**, 457-466.

Valdes M. C., Moreira M., Foriel J. and Moynier F. (2014) The nature of Earth's building blocks as revealed by calcium isotopes. *Earth Planet. Sci. Lett.* **394**, 135-145.

554 Valdes M. C., Debaille V., Berger J. and Armytage R. M. G. (2019) The effects of high-
555 temperature fractional crystallization on calcium isotopic composition. *Chem. Geol.* **509**, 77-
556 91.

557 Wood, B. J. (2000) Phase transformations and partitioning relations in peridotite under lower
558 mantle conditions. *Earth Planet. Sci. Lett.* **174**, 341–354.

559 Zhang H., Wang Y., He Y., Teng F-Z., Jacobsen S. B., Helz R. T., Marsh B. D. and Huang S.
560 (2018). No measurable calcium isotopic fractionation during crystallization of Kilauea Iki
561 Lava Lake. *Geochem. Geophys. Geosyst.* **19**, 3128-3139.

562 Zhao Z., Zhang Z., Huang S., Liu Y., Li X. and Zhang H. (2017) Coupled extremely light Ca
563 and Fe isotopes in peridotites. *Geochim. Cosmochim. Acta* **208**, 368-380.

564 Zheng Y. F. (1997) Prediction of high-temperature oxygen isotope fractionation factors
565 between mantle minerals. *Phys. Chem. Miner.* **24**, 356–364.

566 Figures

567 Figure 1

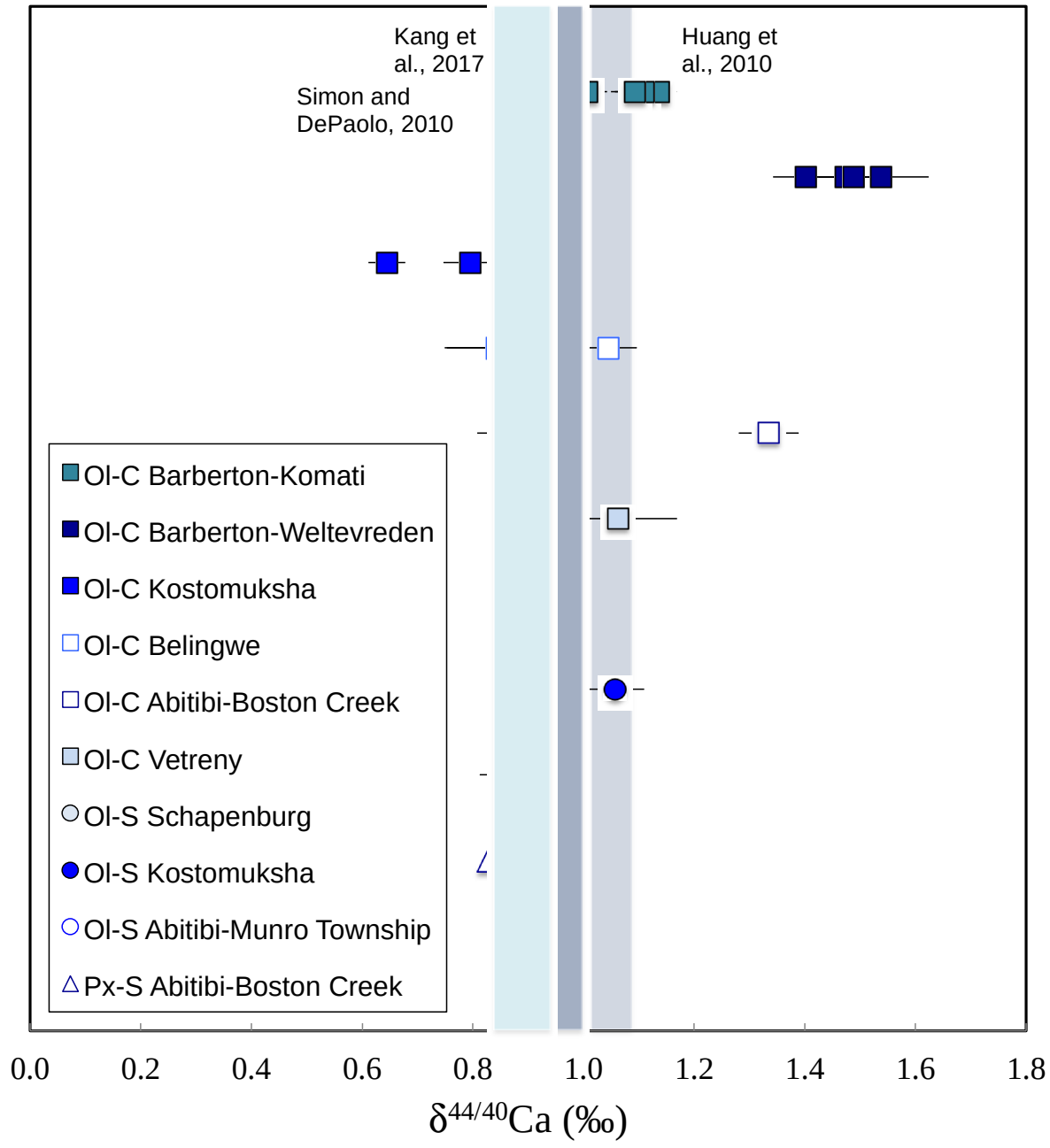
Kang et al., 2017
Simon and DePaolo, 2010
Huang et al., 2010
Ol-C Barberton-Komati
Ol-C Barberton-Weltevreden
Ol-C Kostomuksha
Ol-C Belingwe
Ol-C Abitibi-Boston Creek
Ol-C Vetreny
Ol-S Schapenburg
Ol-S Kostomuksha
Ol-S Abitibi-Munro Township
Px-S Abitibi-Boston Creek
0.0
0.2
0.4
0.6
0.8
1.0
1.2
1.4
1.6
1.8
δ44/40Ca (‰)

Figure 2a

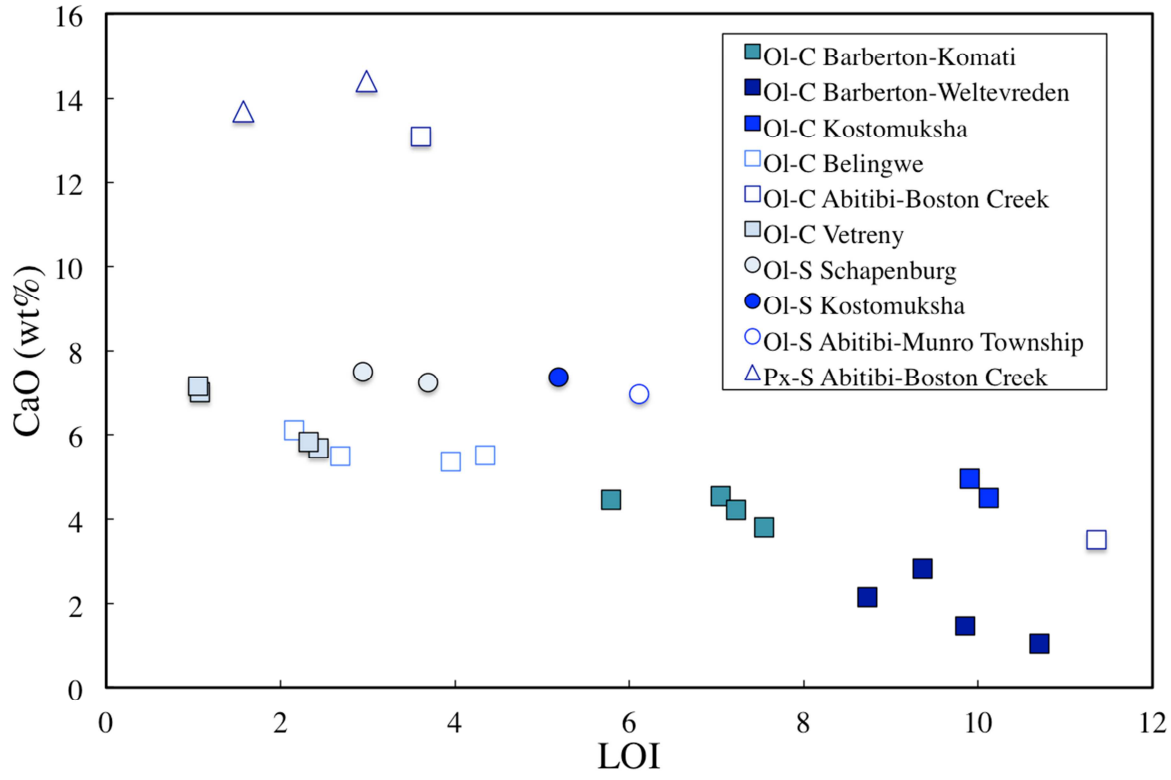

570

571 Figure 2b

572

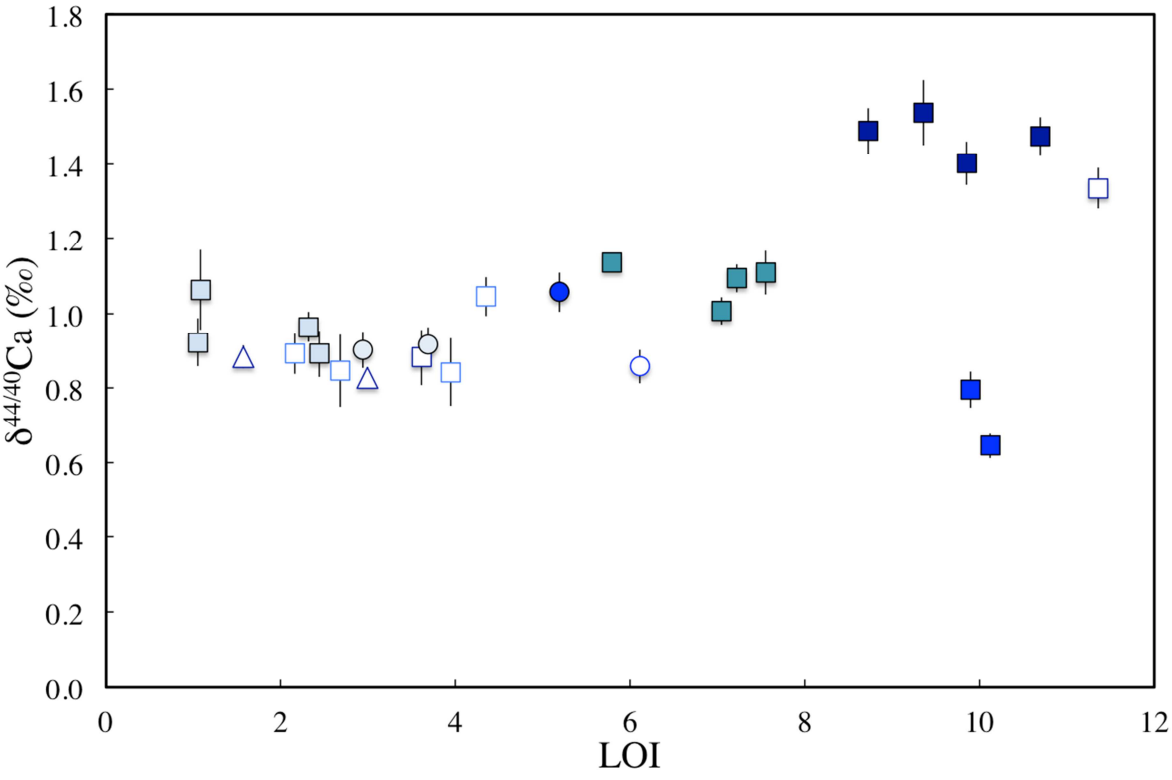

573

574

575 Figure 3

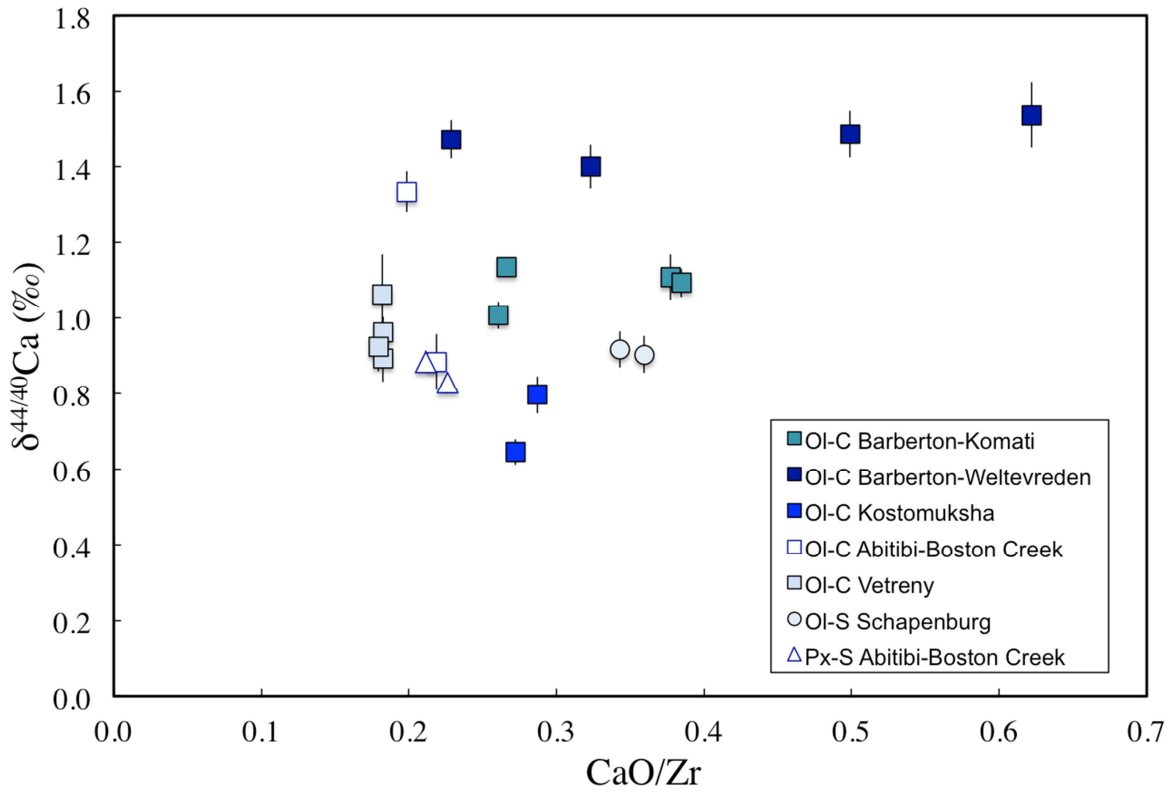

576

577 Figure 4

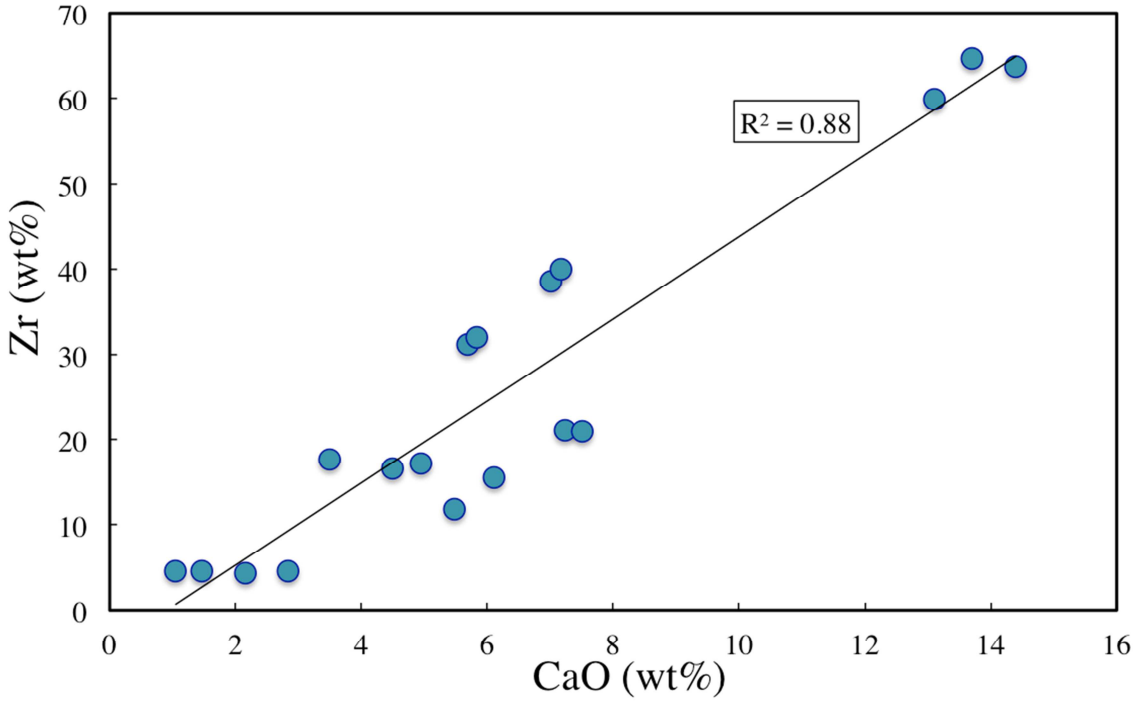

578

579 Figure 5

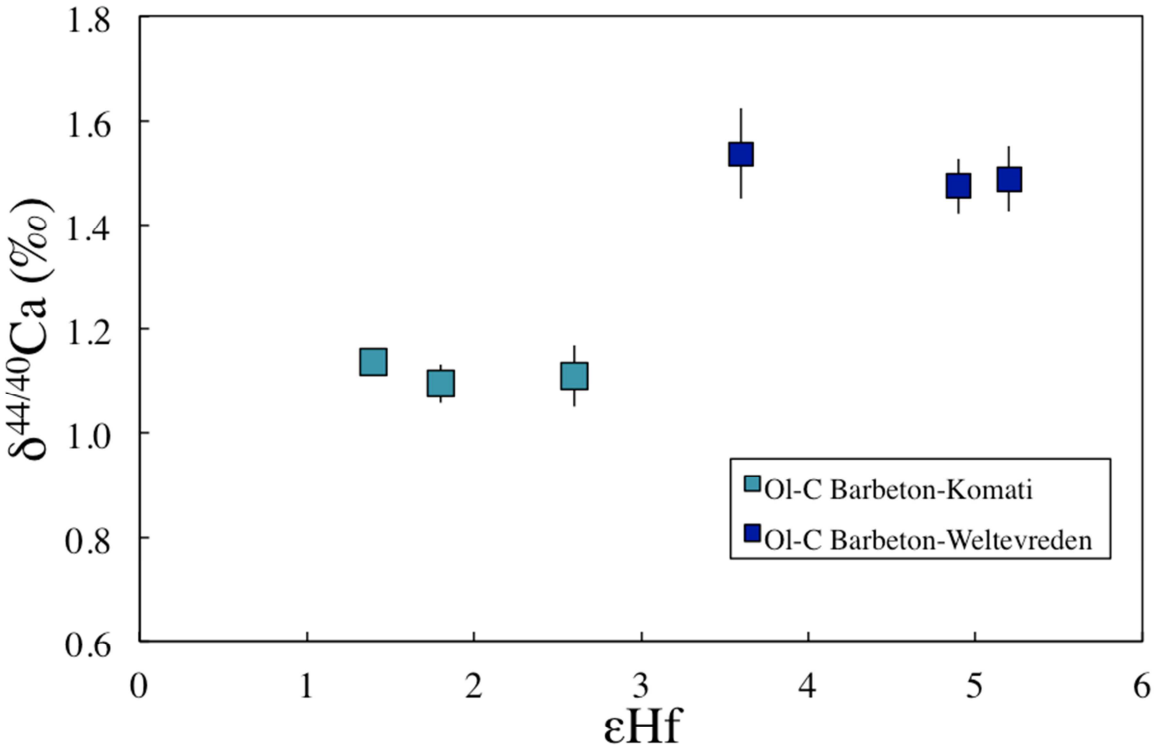

580

581 Figure 6

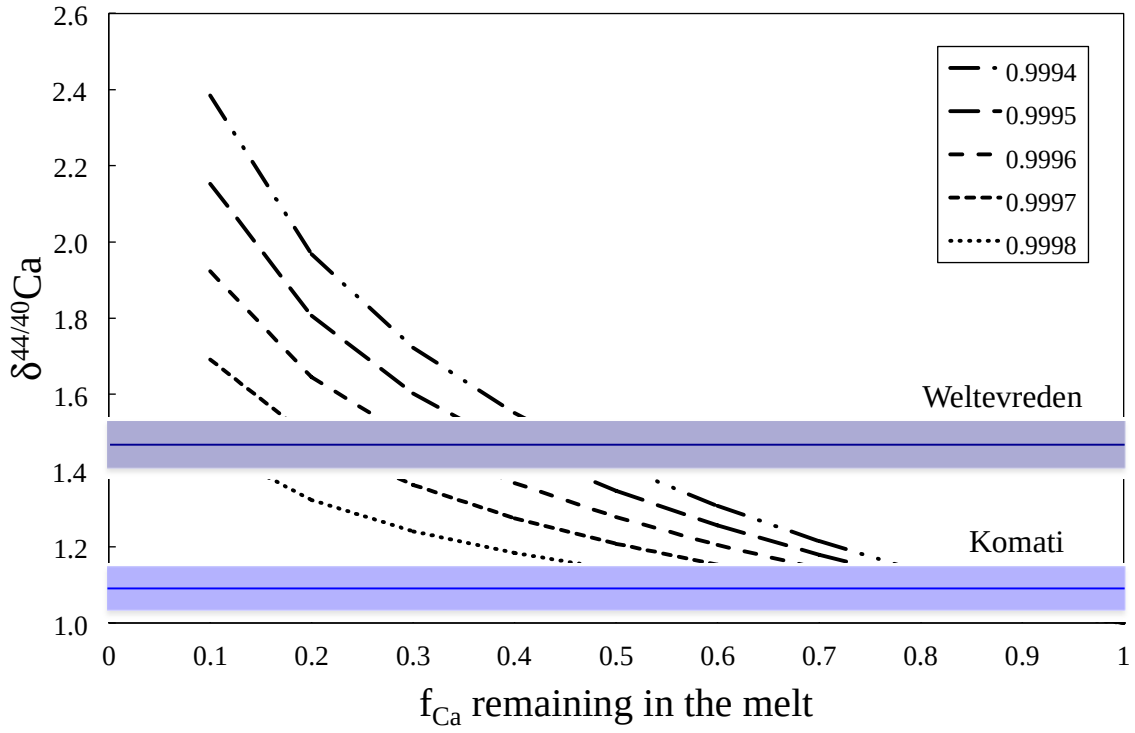

582

583

584 Figure 6a

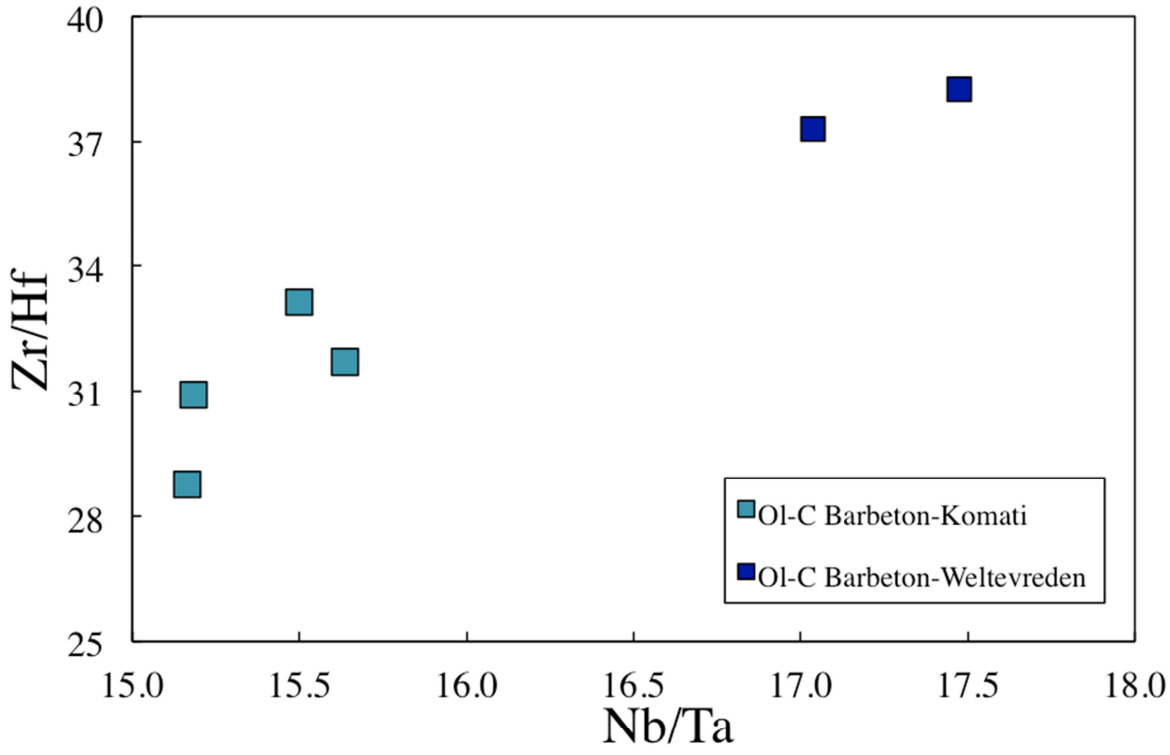

585

586 Figure 6b

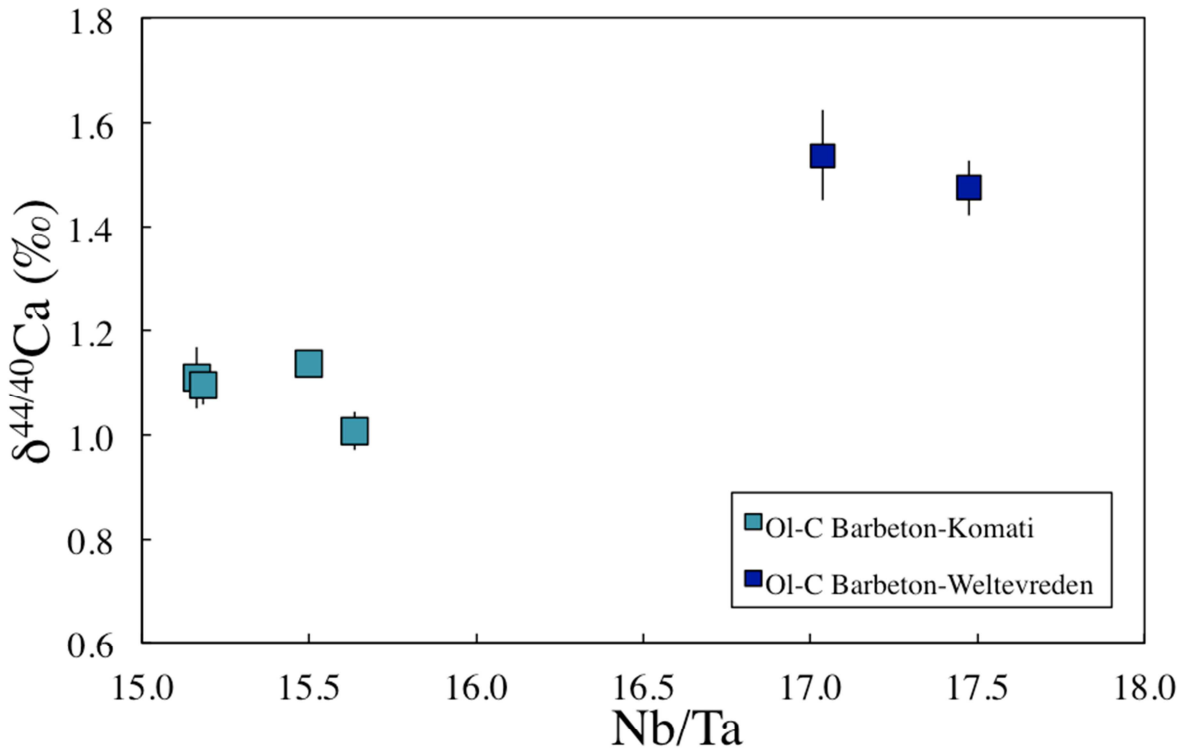

587

588

589 Figure captions

590 Figure 1: Calcium isotopic composition of olivine cumulate (square symbols, Ol-C) and

591 olivine and pyroxene spinifex (circle symbols, Ol-S; triangle symbols, Px-S) textures of

592 komatiites in the study sorted by age with Bartberton the oldest and Vetreny the youngest.

593 The shaded areas represent three estimates of the BSE.

594 Figure 2: a) Calcium isotopic composition and b) CaO content of komatiites relative to their

595 loss of ignition (LOI data from Puchtel et al., 1998; 2013; 2016a; 2016b and 2018).

596 Figure 3: Calcium isotopic composition of komatiites relative to CaO/Zr ratio (CaO and Zr

597 data from Puchtel et al., 1998; 2013; 2016a; 2016b and 2018).

598 Figure 4: Zr content of komatiites relative to their CaO content (data from Puchtel et al.,

599 1998; 2013; 2016a; 2016b and 2018).

Figure 5: Calcium isotopic composition of Barberton komatiites relative to their εHf (data from Puchtel et al., 2013).

Figure 6: A Rayleigh distillation model for the evolution of $\delta^{44/40}Ca$ in the residual liquid during the removal of Ca by crystallization. Five different curves represent the different fractionation factor.

Figure 7a: Nb/Ta of Barberton komatiites relative to their Zr/Hf. The trend reflects fractionation due to perovskite partitioning. Weltevreden komatiites are more exposed to the partitioning than the Komati ones.

Figure 7b: Calcium isotopic composition of Barberton komatiites relative to their Nb/Ta ratio confirming Ca fractionation during perovskite crystallization.

Table 1 - Calcium isotopic composition of komatiites relative to SRM915b and renormalized to SRM915a.

Sample	Location	Texture	Age (Gy)	$\delta^{44/40}Ca$[2]	2se[1]	n[3]
BV03	Komati Fm Barberton Greenstone Belt	Ol-cumulate	3.48	1.14	0.02	4
BV10	Komati Fm Barberton Greenstone Belt	Ol-cumulate	3.48	1.01	0.04	4
BV13	Komati Fm Barberton Greenstone Belt	Ol-cumulate	3.48	1.11	0.06	4
BV15	Komati Fm Barberton Greenstone Belt	Ol-cumulate	3.48	1.09	0.04	4
501-1	Weltevreden Fm Barberton Greenstone Belt	Ol-cumulate	3.26	1.47	0.05	4
501-8	Weltevreden Fm Barberton Greenstone Belt	Ol-cumulate	3.26	1.40	0.06	4
564-2	Weltevreden Fm Barberton Greenstone Belt	Ol-cumulate	3.26	1.49	0.06	4
12-6	Weltevreden Fm Barberton Greenstone Belt	Ol-cumulate	3.26	1.54	0.09	4
94100	Kostomuksha Greenstone Belt	Ol-cumulate	2.82	0.64	0.03	7
94126	Kostomuksha Greenstone Belt	Ol-cumulate	2.82	0.80	0.05	6
TN 17	Belingwe Greenstone Belt	Ol-cumulate	2.7	0.84	0.09	4
TN 18	Belingwe Greenstone Belt	Ol-cumulate	2.7	1.04	0.05	4
TN 19	Belingwe Greenstone Belt	Ol-cumulate	2.7	0.85	0.10	5
ZV 10	Belingwe Greenstone Belt	Ol-cumulate	2.7	0.89	0.05	4
BC06	Boston Creek Abitibi Greenstone Belt	Ol-Px cumulate	2.7	0.88	0.07	7
BC08	Boston Creek Abitibi Greenstone Belt	Ol-cumulate	2.7	1.33	0.05	7
01001	Vetreny Belt Victoria lava lake	Ol-cumulate	2.41	0.89	0.06	4
01104	Vetreny Belt Victoria lava lake	Ol-cumulate	2.41	1.06	0.11	3
01105	Vetreny Belt Victoria lava lake	Ol-cumulate	2.41	0.96	0.04	3
01106	Vetreny Belt Victoria lava lake	Ol-cumulate	2.41	0.92	0.06	7
SCH 2.6	Schapenburg, South Africa	Ol-spinifex	3.55	0.92	0.05	6
SCH 3.6	Schapenburg, South Africa	Ol-spinifex	3.55	0.90	0.05	7
9497	Kostomuksha Greenstone Belt	Ol-spinifex	2.82	1.06	0.05	7
PH08	Abitibi Greenstone Belt Munro Twonship	-	2.7	1.01	0.04	7
PH28	Abitibi Greenstone Belt Munro Twonship	Ol-spinifex	2.7	0.86	0.05	5
BC02	Boston Creek Abitibi Greenstone Belt	Px-spinifex	2.7	0.83	0.03	6
BC03	Boston Creek Abitibi Greenstone Belt	Px-spinifex	2.7	0.88	0.03	7

[1] 2se= 2 x standard deviation /√n

[2] The Ca isotope ratios are normalized relative to SRM 915A

[3] n= number of measurements

611